Microstructural influence on the Cyclic Electro-mechanical Behaviour of Ductile Films on Polymer Substrates

M.J. Cordill[a,*], O. Glushko[a], A. Kleinbichler[a], B. Putz[a], D.M. Többens[c], C. Kirchlechner[a, b]

[a] Erich Schmid Institute of Materials Science, Austrian Academy of Sciences, and Department of Materials Physics, Montanuniversität Leoben, Jahnstrasse 12,
Leoben 8700, Austria

[b] Max-Planck-Institut für Eisenforschung GmbH, Max-Planck-Str.1, 40237 Düsseldorf, Germany

[c] Helmholtz-Zentrum Berlin für Materialien und Energie, Albert-Einstein-Str. 15, 12489 Berlin, Germany

*corresponding author: megan.cordill@oeaw.ac.at

Abstract

When ductile metal films on compliant polymer substrates are strained in tension catastrophic failure can be suppressed by the substrate, thus allowing for their use in flexible electronics and sensors. However, the charge carrying ductile films must be of an optimum thickness and microstructure for the suppression of cracking to occur. Studies of strained films on polymer substrates tend to have more emphasis on the electrical properties and thickness effects than on the film microstructure or deformation behavior. To address both the electrical degradation and deformation behavior of metal films supported by polymer substrates two types of combined electro-mechanical in-situ tests were performed. First, is a combination of in-situ resistance measurements with in-situ confocal scanning laser microscopy imaging of the film surface during cycling. The 4 point probe resistance measurements allow for the examination of the changes in resistance with strain, while the surface imaging permits the visualization of extrusion and crack formation. Second, is the combination of in-situ resistance with in-situ X-Ray diffraction measurements of the film stresses during cycling. The combination of electrical measurements, surface imaging, and stress measurements allow for a complete picture of electro-mechanical behavior needed for the improvement and future success of flexible electronic devices.

Introduction

The lifetime of metal films on polymer substrates is an important parameter to know for flexible electronic applications. However, for flexible electronics, there is still no generally agreed upon failure criteria. Failure criteria for flexible film systems are diverse, and often only use the electric resistance increase of 20-25% [1–4] or an extrusion density saturation based on mechanical damage [5–8] as the hallmark of a failed device. Currently, there is no investigation that examines the correlated electro-mechanical response to determine device lifetime. Without having a universal, or at least clearly defined, failure criteria, researchers and manufactures will not know if certain fabrication methods, such as printing, evaporation or sputtering, are more reliable than others. The fabrication method is important due to the resulting microstructures and interfaces which are responsible for the electro-mechanical behaviour and require more scrutiny.

In the area of metal films on polymer substrates, a vast amount of research has been performed on film thickness effects under monotonic tensile straining [9–12], adhesion [13,14], and cyclic bending or tensile behaviour [9,15–18]. The general trend for film thickness which has been found is that the thinner the film, the higher the yield stress or fracture stress. It has been demonstrated that adhesion is not affected by the film thickness as long as the interface remains the same [12–14]. Brittle adhesion and passivation layers have been shown to be detrimental to the monotonic tensile behaviour [9,19,20]. Under monotonic testing conditions, the brittle adhesion layer formed cracks at strains lower than the overlying ductile film and these initial cracks acted as stress concentration points for further crack development in the ductile film. The influence of brittle adhesion layers under cyclic loading conditions has not been examined yet. However, interlayers can be expected to have very little influence on the behaviour since the maximum strains generally do not exceed more than 2% and the thin brittle adhesion layers may not fail at these low strains. Finally, the film microstructure has not yet been heavily explored even though it is another main contributor to the mechanical and

electrical behaviour. Berger et al. [21] examined the monotonic tensile behaviour of 200 nm Cu films on polyimide substrates with different initial microstructures using in-situ atomic force microscopy (AFM), 4 point probe resistance measurements (4PP) and X-ray diffraction (XRD) experiments. The film with the larger, homogenous grain size did not perform as well as the film with a bi-modal grain size distribution. Further work by Glushko et al. [18] comparing evaporated and inkjet printed Ag lines of the same thickness found that the printed lines with a nanocrystalline microstructure had a longer lifetime than the evaporated lines. It is known that mechanical cycling can lead to extrusion and crack formation as well as grain growth [22–24] in thin ductile films on polymer substrates. These failure mechanisms are dependent on the film thickness, microstructure and interface character. With these findings in mind, the next step would be to study the role of film microstructure and interface character under cyclic loading conditions.

In this study, thin Cu films on polyimide are investigated in the (very) low cycle fatigue regime to determine the electro-mechanical lifetimes. The Cu films have the same thickness but different initial microstructures and interfaces with the substrate. Through the use of novel in-situ-2x (in-situ-squared) [12,25] testing methods, the electrical behaviour can be directly correlated to the mechanical damage induced by the cycling. The combination of two in-situ techniques at the same time allows for a more complete understanding of the role film microstructure has in creating long lasting flexible electronics and sensors. New, well-defined failure criteria will be introduced that use both the electrical and mechanical failure as indicators.

Experimental

Three different thin Cu film systems were produced for testing: an as-deposited 200 nm Cu film, 200 nm film that was annealed at 200 °C for 1 hour after deposition without breaking vacuum, and the third Cu film was produced with a 10 nm Cr interlayer (short form: CuCr). All

films were deposited using electron beam evaporation onto cleaned 50 μm UPILEX brand polyimide (PI) using a deposition rate of 5 Å/s. Straining samples sized 6 mm x 35 mm were cut out of the three different Cu-PI sample sheets using a scalpel. Cyclic tensile testing with in-situ XRD and confocal laser scanning microscopy (CLSM) experiments each with in-situ 4PP, making both types of experiments in-situ-2x, were performed. In-situ CLSM experiments are advantageous over scanning electron microscopy (SEM), AFM or optical microscopy due to the speed of the imaging (approximately 2 minutes per image acquisition) and the larger imaging area with 3-dimensional surface information at a comparable resolution.

All cyclic straining experiments were performed using an Anton Paar TS600 straining stage with resistance probes incorporated into the grips as presented in [25,26]. The order of cyclic straining experiments were implemented in the following manner: one cycle with slow displacement rate (2 μm/s, i.e. strain rate of 10^{-4} s^{-1}), ten cycles with fast loading rate (10 μm/s), one slow cycle, ten fast cycles, one slow cycle, 100 fast cycles, one slow cycle, 100 fast cycles, and one slow cycle for a total of 225 cycles. Each slow cycle consisted of straining to 2% maximum strain, hold for 5 minutes followed by unloading to 0 N. Due to the viscoelastic response of the PI the films are cycled in an almost symmetric manner with plastic strain during the loading and unloading path of the experiment. The fast cycles also went to a maximum strain of 2%, but without the hold and unloading to 2 N. Two different displacement rates were used to make the total time of the experiment manageable (approximately 7 hours). The electrical resistance was recorded throughout all of the mechanical cycling. In-situ CLSM experiments were carried out using the exact same loading conditions and cycle order on an OLS LEXT 4100 confocal laser scanning microscope from Olympus. Images of the same area on the sample surfaces were made before testing, during the hold times of the slow cycles and after every slow cycle or set of cycles. The CLSM images were used to observe the evolution of the deformation and characterize the extrusion spacing.

In-situ XRD straining experiments were performed at the synchrotron source BESSY II (Helmholtz-Zentrum Berlin für Materialien und Energie (HZB), Germany) on the beam line KMC-2 [27] in order to measure the lattice strains and stresses of the Cu films during cyclic tensile straining. The Anton Paar tensile device was positioned so that the sample surface was in reflection geometry with the incoming synchrotron x-ray beam. In-situ measurements during the slow cycles with a beam wavelength of 0.177 nm and a beam diameter of 300 µm were continuously performed at five different ψ angles using a Bruker VÅNTEC 2000 area detector and an exposure time of 5 s. Lattice strains were analyzed by the $\sin^2 \Psi$ method [28] ($\sin^2 \Psi$ range 0-0.6 (-)) in the direction of the applied tensile strain. For this, peak positions and peak widths were derived by fitting a Pearson VII function. Film stresses were calculated using X-ray elastic constants (XECs) (1/2 S_2) [29] for untextured (111) Cu reflections. XECs were calculated from single-crystal elastic constants assuming the Hill model with the software ElastiX [30]. From these experiments, stress-strain curves averaged over the beam footprint on the sample are calculated using Hooke's law, where the Cu film stresses obtained by the synchrotron data are plotted against the engineering strains measured with the tensile device. The residual lattice strains were measured prior to and after every cycle or set of cycles with high resolution at 11 different Ψ angles. The Cr interlayer (10 nm) was too thin to provide a sufficient signal for $\sin^2 \Psi$ analysis and was not used.

The grain size of the three films before and after cyclic straining was characterized using SEM (Zeiss LEO 1525) and the TSL OIM Data Collection (version 5.31) with electron backscatter diffraction (EBSD) scans. Three EBSD scans were made on each film and the grain size and texture were determined. Figure 1 displays representative EBSD images of the three films. For the as-deposited film only pixels that could be indexed are shown in colour (Figure 1a). The measured average grain sizes weighted by area are: As-deposited: 380±130 nm; Annealed 695±200nm; CuCr 800±250nm. All three films were previously strained with monotonic loading to 12% strain with in-situ XRD to determine the mechanical behaviour

[9,21]. The measured yield stresses for the three films were determined as: As-deposited: 900 MPa; Annealed 750 MPa; CuCr 850 MPa.

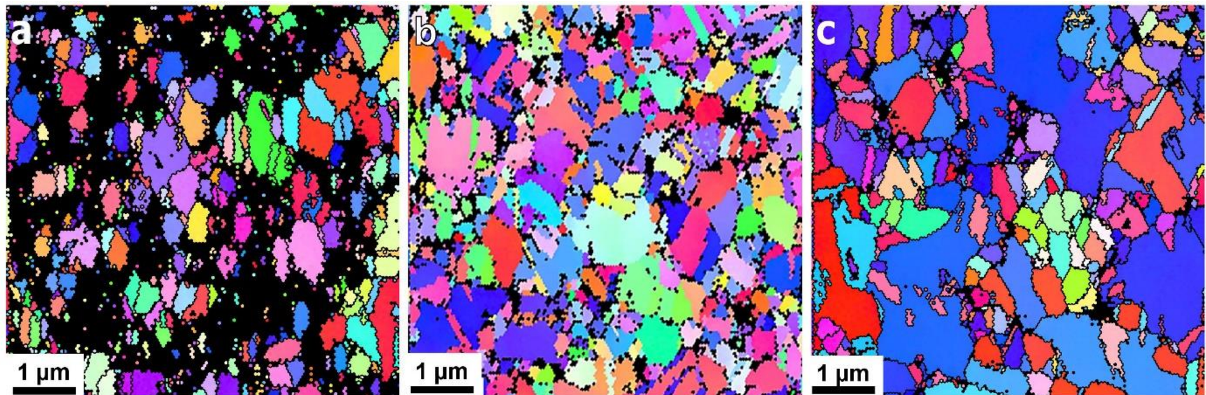

Figure 1: EBSD images of the (a) as-deposited 200 nm Cu film, (b) annealed 200 nm Cu film, and (c) as-deposited 200 nm Cu with a 10 nm Cr interlayer before cyclic tensile straining. (Colour online)

Results

The cyclic in-situ-2x 4PP-CLSM experiments were ideal to observe the evolution of the surface damage and resistance with increasing cycle number. Figure 2 illustrates the surface damage and relative resistance ratios (R/R_0) as a function of cycling of the three different films. After the first cycle, the CuCr film already exhibited surface damage in the form of localized necking (not shown). At the end of 12 cycles (Figure 2a-c) still only the CuCr film had surface damage in the form of localized necks. Necks were identified as drops in surface profiles extracted from the CLSM height images, which are not shown. Figure 2 shows only the CLSM laser images which better illustrate the surface damage. It should be noted that the dark spots in the CLSM images of the annealed Cu film (Figure 2b) are residual native oxide islands that could not be removed prior to testing. The resistance of the three films after 12 cycles is shown in Figure 2d. The as-deposited Cu film's R/R_0 remains relatively constant, while it increases slightly for the annealed Cu and CuCr films. All films would be considered electrically viable (not failed) at this stage since the R/R_0 values (maximum or minimum) do not increase over 20%, but mechanically the CuCr film has reached an extrusion spacing saturation level (Figure 3a). It should be noted that that R/R_0 of the annealed Cu film is increasing more than the CuCr

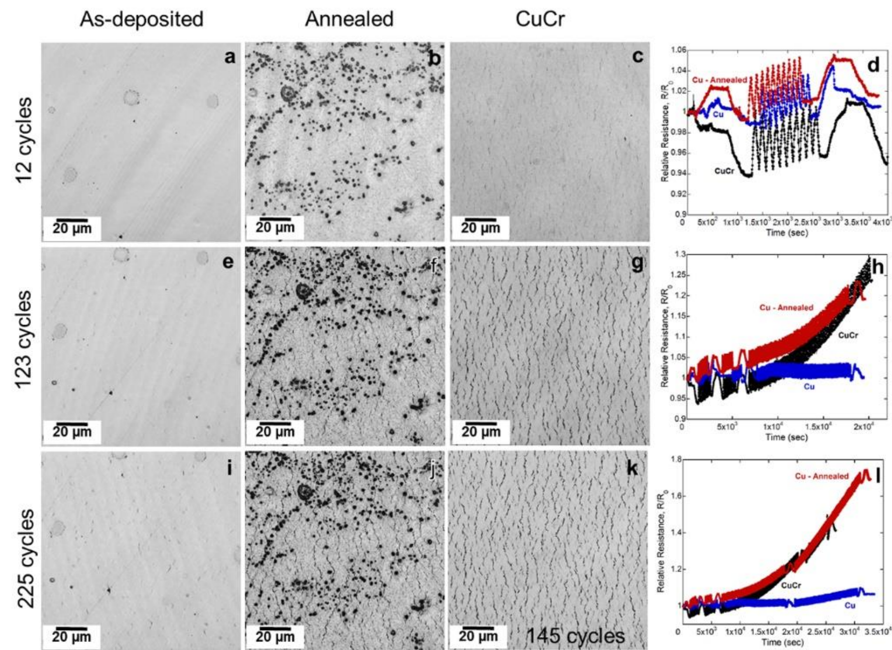

Figure 2: CLSM laser images taken during mechanical cycling for all three film systems with the corresponding R/R_0 measurements. (a-c) after 12 cycles, (e-g) after 123 cycles, and (i-k) after 225 (or 145 for CuCr). The R/R_0 curves as a function of time recorded during the in-situ experiment are shown in (d, h, and l). Surface damage was observed after the first cycle in the CuCr system, while observed after 123 cycles in the as-deposited and annealed systems. (Colour online)

and is due to the normalization of the resistance with in the initial resistance, R_0. In this case, the CuCr has a significantly higher R_0 value than the annealed Cu and the impact of the change in resistance is smaller in the CuCr making the increase in the R/R_0 somewhat later than the annealed Cu film. Therefore, the overall R/R_0 trends of the three different films are the important result rather than the direct comparisons between the three films. Figure 2e-g shows the surface damage after the films were subjected to another 111 cycles (total 123 cycles). The as-deposited Cu film exhibits some localized necking that is widely spaced, the annealed Cu film has extensive necking and/or extrusion formation, and the CuCr film surface damage has more connected extrusions and cracks. The R/R_0 data after 123 cycles (Figure 2h) indicates that the as-deposited Cu film still has a constant average R/R_0 while for the annealed Cu and CuCr films R/R_0 has increased to above the 20% failure threshold. For the next set of cycles, the as-deposited and annealed Cu films were further cycled 100 times, while for the CuCr film only

another 24 cycles were performed due to a programming error. The as-deposited Cu film illustrates more, but still highly localized damage (Figure 2i). Increased deformation of the annealed Cu is observed in Figure 2j with more connected extrusions. The damage of the CuCr film is similar to the damage after 123 cycles (Figure 2k). At this point, only the as-deposited Cu film is still electrically viable as the R/R_0 ratio is about 1.1 (equal to only a 10% increase of resistance) (Figure 2l). The extrusion spacing evolution and the average R/R_0 ratios for all three films are shown in Figure 3. Interestingly, the extrusion spacings remain constant with cycle number, with the exception of the as-deposited Cu, and even though the thickness of the Cu is the same for all three samples, the extrusion spacings are quite different.

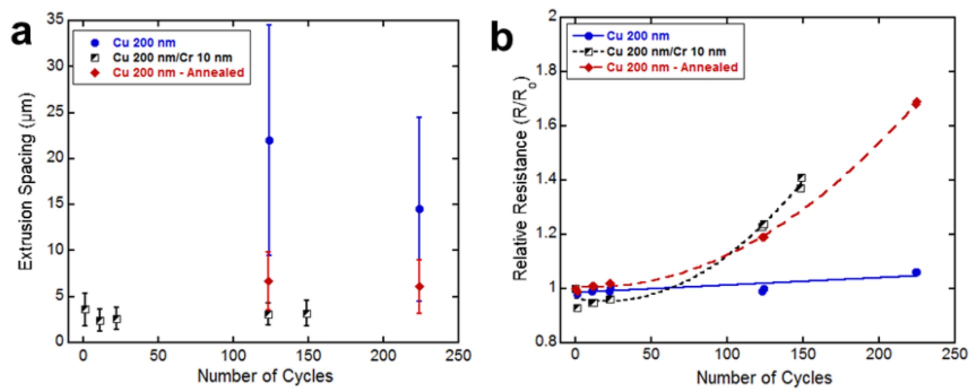

Figure 3: (a) Measured extrusion spacings a function of cycles for the three different Cu films. On the 200 nm Cu film with 10 nm Cr interlayer system, extrusions were observed after 1 cycle and the spacing saturated after 10 more cycles. After 123 cycles, extrusions formed in the annealed Cu film and also reached saturation immediately. (b) Average R/R_0 of the three different films to more clearly illstrate the increase of the resistance with cycling. The lines are only used to guide the eye and have no mathematical meaning. (Colour online)

The in-situ XRD experiments were used to determine the stress development in the Cu films during straining and the stress state after cycling (in the unloaded state). Recall that the 1st, 11th, 23rd, and 124th cycles were performed slowly (2 µm/s) to allow the continuous in-situ XRD measurement for each film. Figure 4a illustrates the measured stress during straining to 2% of the as-deposited Cu film. It is important to note that the film undergoes tensile stresses during loading and compression stresses during unloading, which are both necessary for extrusions to develop. After the initial cycle the stress hysteresis slightly decreases, but after

the 11th cycle (2nd in-situ XRD cycle) the hysteresis loops of higher cycle numbers match. As shown in Figures 4b and 4c, a similar behaviour (tension-compression, hysteresis loop decreases) was observed for the annealed Cu film and the CuCr film, respectively. When all three films are shown together (Figure 4d), it is clearly observed that the CuCr film has a larger hysteresis than the films without the Cr interlayer. The as-deposited and annealed Cu films have a very similar stress response. The larger hysteresis curves of the CuCr is most likely due to the Cr interlayer which acts as a hard interface to dislocation motion and the results are similar to those found by Xiang and Vlassak [31] using bulge testing on passivated and unpassivated films.

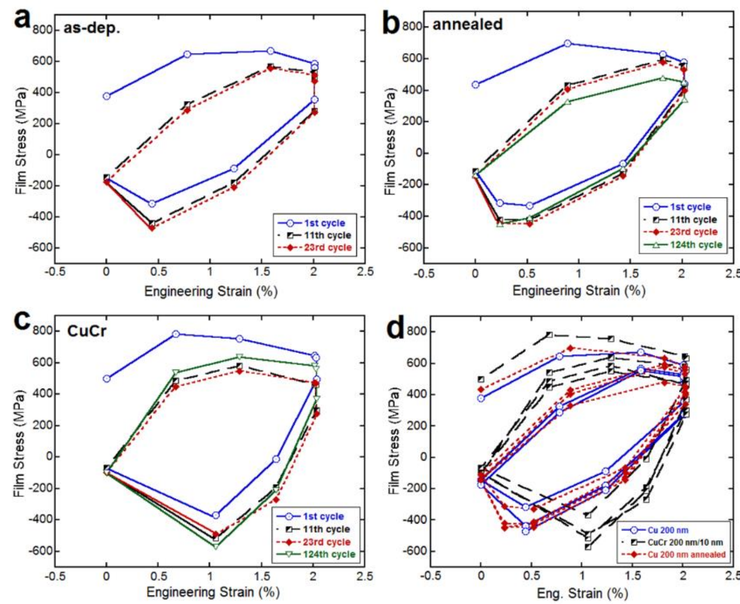

Figure 4: Film stresses meaured in-situ during the slow straining cycles for the (a) 200 nm as-deposited Cu film, (b) 200 nm annealed Cu film, and (c) 200 nm Cu film with 10 nm Cr interlayer. (d) Direct comparison of the three different films illustrating the larger hystersis of the CuCr film system. (Colour online)

After every slow cycle or set of faster cycles a high resolution measurement of the lattice strain was performed (Figure 5). The initial lattice strains of the three different films were approximately the same with a value of about 0.1% tensile. After one straining cycle to 2%, the lattice strains drop significantly to about 0.2% compressive. With further cycling, the lattice strains of all three films reach a plateau at slightly above 0.4% strain compressive with the CuCr

film always being slightly lower until 225 cycles. During the in-situ XRD experiment, the annealed Cu film broke during the 2nd set of 100 cycles and no final XRD measurements could be performed. It is difficult to formulate a failure criterion based only on the lattice strain measurement, however, the 4PP resistance data measured during the XRD experiments was very similar to that measured during the in-situ CLSM experiments and could be used to determine the electrical failure.

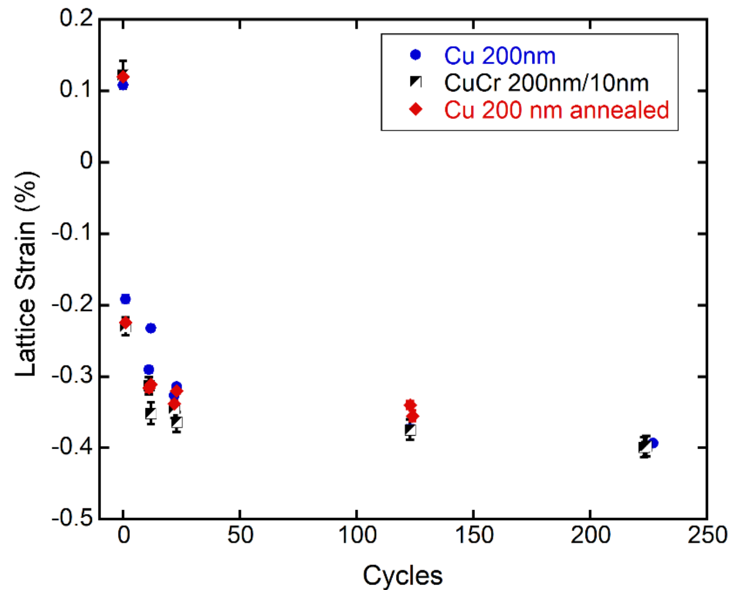

Figure 5: Evolution of the Cu lattice strains measured after each single slow cycle or set of faster cycles. All three Cu films show approximately the same behavior. (Colour online)

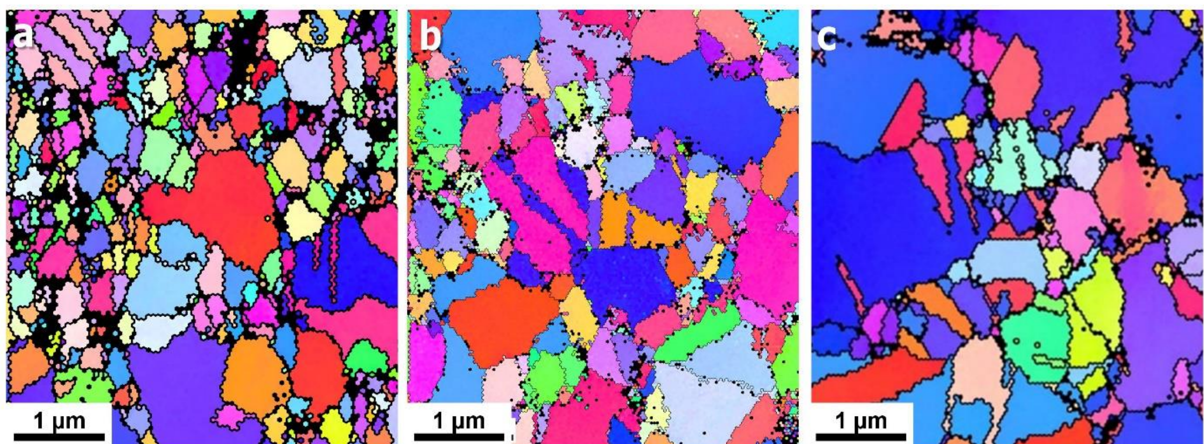

Figure 6: EBSD images of the (a) as-deposited 200 nm Cu film, (b) annealed 200 nm Cu film, and (c) as-deposited 200 nm Cu with a 10 nm Cr interlayer after 225 applied 2% tensile straining cycles. Compared to Figure 1, grain growth is observed in the as-deposited film (a). (Colour online)

The grain size of the as-deposited Cu film did increase slightly during the 225 cycles to 490±150 nm (Figure 6a). This cyclic grain growth has been observed before in the same film system and in Au films on polyimide [22,23]. Figure 6b and 6c are EBSD images after cycling of the annealed Cu and CuCr films, respectively. The grain sizes do not significantly change with cycling (Annealed: 650±200 nm; CuCr: 910±260 nm).

Discussion

Through the combination of electrical resistance measurements, CLSM surface imaging and XRD stress measurements, a clearer idea about how the film microstructure and the metal-polymer interface influence the lifetime of ductile conducting layers used in flexible electronics was developed. First, the brittle interlayers do not help to enhance the mechanical stability and actually cause cracks and extrusions to form even at very low levels of strain [9,20]. The CuCr film showed damage already after the first cycle. Granted, the initial damage was only localized necking, but the initial necking developed into extrusions and through thickness cracks with continued cycling. This was illustrated by the immediate extrusion spacing saturation. The evolution of the CuCr surface damage shown in Figure 2 demonstrates that not only the extrusion spacing is important, but also the length of the extrusions [32]. Only when the necks and extrusions became a complete network over the sample width was the R/R_0 observed to increase over 20%. After less than 123 cycles, the CuCr would be considered electrically failed and was closely followed by the annealed Cu film at about 150 cycles. The annealed Cu film has a large and homogeneous initial grain size compared to the as-deposited Cu and CuCr. This large and homogeneous grain size is most likely the reason behind the observed early electro-mechanical failure. With large grains, dislocations can move more easily compared to small grains and the slip is more localized as soon as dislocations have a path where they can glide, similar to the findings observed in Au films under cyclic bulge testing [24]. The annealed Cu extrusion spacing also reached a constant value immediately, similar to the CuCr, with the

extrusion network forming much faster over the sample width. The as-deposited Cu film did not electrically fail after the maximum applied cycle number of 225 cycles because the relative resistance ratio did not increase above 20%. Even though damage is present, the spacing has not yet reached a constant value as observed for the annealed Cu and CuCr films. The difference is the absence of a Cr interlayer and a bi-modal microstructure. The combination of the bi-modal microstructure without an adhesion interlayer allows for grain growth without stress concentrations from interlayer cracks. With the bi-modal microstructure, grain growth occurs until a more homogenous grain size is reached and only then will extrusions and cracks initiate in the large grains without the influence of an underlying Cr adhesion layer. The XRD experiments support these conclusions. In the early cycling stages, the residual lattice strains of the as-deposited film were slightly higher compared to the annealed Cu film and the CuCr film (Figure 5). When the lattice strains for all three films converge at 123 cycles, damage is finally observed in the as-deposited film (Figure 3a) and could indicate that grain growth is complete. A more detailed experiment examining the grain growth with XRD was attempted, however, the results were inconclusive. The large error bars of the extrusion spacing of the as-deposited Cu film shown in Figure 3 illustrate that the damage is widely spaced and would still need at least 100-200 more cycles to reach saturation and electrical failure. Ductile conducting lines should be fabricated so that they have a metastable [22] or nanocrystalline microstructure [23] which can grow when subjected to cyclic strain in order to improve the device lifetime.

Through the use of combined in-situ methods, new definitions of failure can be presented. For example, the extrusion spacing reaches saturation well before the resistance growth exceeds 20%. This means that the saturation of the extrusion spacing is the lower bound of the lifetime and the electrical resistance ratio the upper bound. The saturation of the extrusion spacing is an indication that the pathways for plastic deformation are set and with further cycling will only continue to form through thickness cracks detrimental to the electro-mechanical behaviour. Comparison of XRD and CLSM show that the saturation of the residual

lattice strain also correlates well with the saturation of the extrusion spacing and can, therefore, also act as a lower bound. When the extrusion spacing and electrical resistance increase converge at the same number of cycles, as most likely in the case of the as-deposited film, then an accurate lifetime can be determined which is based on informed electrical and mechanical failure mechanisms.

Conclusions

Multiple in-situ methods were used to examine the combined electro-mechanical behaviour of metal-polymer systems under cyclic tensile loading. The low cycle fatigue regime was investigated with in-situ 4PP-CLSM and 4PP-XRD measurements to directly correlate the electrical resistance with the mechanically induced damage and the evolution of the film stress. Three 200 nm Cu films with different microstructures and interfaces were examined to determine which film has the longer lifetime based on the electrical failure criteria (R/R_o increase of 20%) and the extrusion spacing. It was found that a bi-modal (metastable) Cu microstructure without a brittle interlayer outperforms a large homogenous microstructure (about 1 µm sized grains) and a Cu film with a Cr interlayer by at least 100 cycles. The bi-modal structure must first stabilize the grains through grain growth and then plastic deformation can build-up in the film, causing extrusions and cracks to form. Combined failure criteria are introduced using both the extrusion spacing saturation and the relative resistance increase. If the extrusion spacing reaches saturation before the relative resistance increases above 20%, a lower bound of the lifetime is determined. If the two criteria (saturation extrusion spacing and relative resistance increase) converge at the same cycle number, then an accurate determination of the lifetime can be documented. It has also been shown that it is best to combine electrical and mechanical observation methods to be better informed about the failure of these complex material systems.

Acknowledgements

Funding of the research has been provided by the Austrian Science Foundation (FWF) through project P22648-N20. The authors would like to thank the HZB for the allocation of synchrotron radiation beam time and thankfully acknowledge the financial support by the HZB (project no. 14201169-ST). The authors would like to thank J. Schalko of the Research Unit for Integrated Sensor Systems of the Austrian Academy of Sciences (Wiener Neustadt, Austria) for providing the Cu films. The confocal laser scanning microscopy images were made possible through a 2014 Olympus Technology Grant.

References

[1] G.D. Sim, Y. Hwangbo, H.H. Kim, S.B. Lee, J.J. Vlassak, Fatigue of polymer-supported Ag thin films, Scr. Mater. 66 (2012) 915–918. doi:10.1016/j.scriptamat.2012.02.030.

[2] G.-D. Sim, Y.-S. Lee, S.-B. Lee, J.J. Vlassak, Effects of stretching and cycling on the fatigue behavior of polymer-supported Ag thin films, Mater. Sci. Eng. A. 575 (2013) 86–93. doi:10.1016/j.msea.2013.03.043.

[3] X.J. Sun, C.C. Wang, J. Zhang, G. Liu, G.J.P. Zhang, X.D. Ding, et al., Thickness dependent fatigue life at microcrack nucleation for metal thin films on flexible substrates, J. Phys. D. Appl. Phys. 41 (2008) 195404. doi:10.1088/0022-3727/41/19/195404.

[4] J.Y. Zhang, X. Zhang, G. Liu, R.H. Wang, G.J. Zhang, J. Sun, Length scale dependent yield strength and fatigue behavior of nanocrystalline Cu thin films, Mater. Sci. Eng. A. 528 (2011) 7774–7780. doi:10.1016/j.msea.2011.06.083.

[5] D. Wang, C.A. Volkert, O. Kraft, Effect of length scale on fatigue life and damage formation in thin Cu films, Mater. Sci. Eng. A. 493 (2008) 267–273. doi:10.1016/j.msea.2007.06.092.

[6] R. Schwaiger, G. Dehm, O. Kraft, Cyclic deformation of polycrystalline Cu films, Philos. Mag. 83 (2003) 693–710. doi:10.1080/0141861021000056690.

[7] S. Eve, N. Huber, A. Last, O. Kraft, Fatigue behavior of thin Au and Al films on polycarbonate and polymethylmethacrylate for micro-optical components, Thin Solid Films. 517 (2009) 2702–2707. doi:10.1016/j.tsf.2008.12.018.

[8] O. Kraft, P. Wellner, M. Hommel, R. Schwaiger, E. Arzt, Fatigue behavior of polycrystalline thin copper films, Zeitschrift Fuer Met. Res. Adv. Tech. 93 (2002) 392–400.http://www.scopus.com/scopus/inward/record.url?eid=2-s2.0-0036571736&partnerID=40&rel=R5.6.0.

[9] V.M. Marx, F. Toth, A. Wiesinger, J. Berger, C. Kirchlechner, M.J. Cordill, et al., The influence of a brittle Cr interlayer on the deformation behavior of thin Cu films on flexible substrates: Experiment and model, Acta Mater. 89 (2015) 278–289. doi:10.1016/j.actamat.2015.01.047.

[10] P.A. Gruber, J. Böhm, F. Onuseit, A. Wanner, R. Spolenak, E. Arzt, Size effects on yield strength and strain hardening for ultra-thin Cu films with and without passivation: A study by synchrotron and bulge test techniques, Acta Mater. 56 (2008) 2318–2335. doi:10.1016/j.scriptamat.2012.04.018.

[11] A. Wyss, M. Schamel, A.S. Sologubenko, R. Denk, M. Hohage, P. Zeppenfeld, et al., Reflectance anisotropy spectroscopy as a tool for mechanical characterization of metallic thin films, J. Phys. D. Appl. Phys. 48 (2015) 415303-1–11. doi:10.1088/0022-3727/48/41/415303.

[12] T. Jörg, M.J. Cordill, R. Franz, C. Kirchlechner, D.M. Többens, J. Winkler, et al., Thickness dependence of the electro-mechanical response of sputter-deposited Mo thin films on polyimide: Insights from in situ synchrotron diffraction tensile tests, Mater. Sci. Eng. A. 697 (2017) 17–23. doi:10.1016/j.msea.2017.04.101.

[13] M.J. Cordill, F.D. Fischer, F.G. Rammerstorfer, G. Dehm, Adhesion energies of Cr thin films on polyimide determined from buckling: Experiment and model, Acta Mater. 58 (2010) 5520–5531. doi:10.1016/j.actamat.2010.06.032.

[14] S. Frank, U.A. Handge, S. Olliges, R. Spolenak, The relationship between thin film fragmentation and buckle formation: Synchrotron-based in situ studies and two-dimensional stress analysis, Acta Mater. 57 (2009) 1442–1453. doi:10.1016/j.actamat.2008.11.023.

[15] B.J. Kim, H.A.S. Shin, J.H. Lee, T.Y. Yan, T. Haas, P. Gruber, et al., Effect of film thickness on the stretchability and fatigue resistance of Cu films on polymer substrates, J. Mater. R. 29 (2014) 2827–2834. doi:10.1557/jmr.2014.339.

[16] P.A. Gruber, S. Olliges, E. Arzt, R. Spolenak, Temperature dependence of mechanical properties in ultrathin Au films with and without passivation, J. Mater. Res. 23 (2008) 2406–2419. doi:10.1557/jmr.2008.0292.

[17] J. Lohmiller, R. Spolenak, P.A. Gruber, Alloy-dependent deformation behavior of highly ductile nanocrystalline AuCu thin films, Mater. Sci. Eng. A. 595 (2014) 235–240. doi:10.1016/j.msea.2013.12.021.

[18] O. Glushko, A. Klug, E.J.W. List-Kratochvil, M.J. Cordill, Monotonic and cyclic mechanical reliabiltiy of metallization lines on polymer substrates, J. Mater. Res. 32 (2017) 1760–1769.

[19] P.A. Gruber, E. Arzt, R. Spolenak, Brittle-to-ductile transition in ultrathin Ta/Cu film systems, J. Mater. Res. 24 (2009) 1906–1918. doi:10.1557/jmr.2009.0252.

[20] B. Putz, R.L. Schoeppner, O. Glushko, D.F. Bahr, M.J. Cordill, Improved electro-mechanical performance of gold films on polyimide without adhesion layers, Scr. Mater. 102 (2015) 23–26. doi:10.1016/j.scriptamat.2015.02.005.

[21] J. Berger, O. Glushko, V.M. Marx, C. Kirchlechner, M.J. Cordill, Effect of microstructure on the electro-mechanical behavior of Cu films on polyimide, JOM. 68 (2016) 1640–1646. doi:10.1007/s11837-016-1940-z.

[22] O. Glushko, M.J. Cordill, Electrical Resistance Decrease Due to Grain Coarsening Under Cyclic Deformation, JOM. 66 (2014) 1–4. doi:10.1007/s11837-014-0943-x.

[23] O. Glushko, A. Klug, E.J.W.J.W. List-Kratochvil, M.J. Cordill, Relationship between mechanical damage and electrical degradation in polymer-supported metal films subjected to cyclic loading, Mater. Sci. Eng. A. 662 (2016) 157–161. doi:10.1016/j.msea.2016.03.052.

[24] B. Merle, M. Göken, Bulge fatigue testing of freestanding and supported gold films, J. Mater. Res. 29 (2014) 267–276. doi:10.1557/jmr.2013.373.

[25] B. Putz, O. Glushko, V.M. Marx, C. Kirchlechner, D. Többens, M.J. Cordill, Electro-mechanical performance of thin gold films on polyimide Barbara, MRS Adv. 1 (2016) 773–778. doi:10.1557/adv.2016.

[26] M.J. Cordill, O. Glushko, B. Putz, Electro-Mechanical Testing of Conductive Materials Used in Flexible Electronics, Front. Mater. 3 (2016) 1–11. doi:10.3389/fmats.2016.00011.

[27] Helmholtz-Zentrum Berlin für Materialen und Energie, KMC-2: an X-ray beamline with dedicated diffraction and XAS endstations at BESSY II, J. Large-Scale Res. Facil. JLSRF. 2 (2016) 1–6. doi:10.17815/jlsrf-2-65.

[28] L. Spieß, G. Teichert, R. Schwarzer, H. Behnken, C. Genzel, Untersuchungen an dünnen Schichten, in: Mod. Röntgenbeugung SE - 13, Vieweg+Teubner, 2009: pp. 453–486. doi:10.1007/978-3-8349-9434-9_13.

[29] I.C. Noyan, J.B. Cohen, Residual stress: measurement by diffraction and interpretation, Springer-Verlag, New York, 2013.

[30] H. Wern, N. Koch, T. Maas, Selfconsistent calculation of the x-ray elastic constants of polycrystalline materials for arbitrary crystal symmetry, in: Mater. Sci. Forum, 2002: pp. 127–132.http://www.scopus.com/inward/record.url?eid=2-s2.0-0036433960&partnerID=tZOtx3y1.

[31] Y. Xiang, J.J. Vlassak, Bauschinger and size effects in thin-film plasticity, Acta Mater. 54 (2006) 5449–5460. doi:10.1016/j.actamat.2006.06.059.

[32] O. Glushko, P. Kraker, M.J. Cordill, Explicit relationship between electrical and topological degradation of polymer-supported metal films subjected to mechanical loading, Appl. Phys. Lett. 110 (2017) 191904.